Assessment of Inter- and Intrapatient Variability in $C^{15}O_2$ Positron Emission Tomography Measurements of Blood Flow in Patients with Intra-abdominal Cancers

Paula Wells, Terry Jones, and Pat Price

Department of Cancer Medicine, MRC Cyclotron Unit, Imperial College London, Hammersmith Hospital, Hammersmith, London, United Kingdom

ABSTRACT

Purpose: **The aim of the study was to evaluate the inter- and intrapatient variability of positron emission tomography (PET) measurements of perfusion in advanced solid cancers.**

***Experimental Design*: Thirty-seven patients with predominantly intra-abdominal tumors underwent PET imaging using inhaled $C^{15}O_2$. Repeat data were obtained by scanning five patients twice, 1 week apart, with no intervening therapy. Regional flow and the volume of distribution (V_d) were measured from dynamic images by use of a one-compartment model. Inter- and intrapatient variability were measured as the coefficient of variability (CV). Data were also obtained for regions of interest in normal liver, spleen, and kidney.**

Results: **The mean (±SD) regional flow in the tumors was 0.46 ± 0.19 $ml_{blood}/min/ml_{tissue}$, and the mean V_d was 0.74 ± 0.15 ml_{blood}/ml_{tissue}. Variability in tumor flow was greater between ($n = 37$; CV = 41%) than within ($n = 5$; CV = 11%) patients. Variability in tumor V_d was greater between (CV = 21%) than within (CV = 6%) patients. There was a good correlation between the repeat tumor data for both regional flow ($\rho = 0.82$; $P = 0.023$) and V_d ($\rho = 0.89$; $P = 0.007$). Normal tissue variability was also greater between than within patients. In all cases, no statistically significant differences were seen between repeat measurements in the same patient.**

Conclusions: **Dynamic $C^{15}O_2$ PET measurements of regional flow are reproducible in patients with predominantly intra-abdominal malignancies and may be useful for the pharmacodynamic evaluation of novel antivascular and antiangiogenic cancer therapeutic agents.**

Received 4/15/03; revised 9/11/03; accepted 9/22/03.

Grant support: Medical Research Council of the United Kingdom and Cancer Research United Kingdom Grants C153/A1797 and C153/A1802.

The costs of publication of this article were defrayed in part by the payment of page charges. This article must therefore be hereby marked *advertisement* in accordance with 18 U.S.C. Section 1734 solely to indicate this fact.

Requests for reprints: Pat Price, Academic Department of Radiation Oncology, Wolfson Molecular Imaging Centre, Christie NHS Trust Hospital, Wilmslow Road, Manchester M20 4BX, United Kingdom. Phone: 44-161-446-8003; Fax: 44-446-161-8111; E-mail: Anne.Mason@man.ac.uk.

INTRODUCTION

The measurement of vascular physiology and hemodynamic parameters is a growing area of cancer research that is linked with the development of drugs that target the tumor vasculature. This is because the maximum tolerated dose used for dose and schedule-finding studies of conventional antiproliferative chemotherapeutic agents may be less applicable in antiangiogenic/vascular approaches. The lack of antiproliferative toxicity associated with these new agents has led to interest in the use of surrogate endpoints of efficacy that could be used in their early clinical evaluation. One of the rationales behind the development of functional imaging of vascular physiology in cancer research, therefore, is to provide pharmacodynamic methods that can be applied in Phase I/II studies of antiangiogenic/vascular drugs. Several endpoints are of interest that include the measurement of tumor blood flow.

The principle underlying positron emission tomography (PET) measurements of tumor blood flow is that the transcapillary exchange of a freely diffusible, biologically inert, and nonmetabolized tracer is limited by blood flow and not by diffusion or metabolism (1, 2). With a constant infusion of a short-lived isotope, its concentration in a tissue at equilibrium is related to blood flow. The first quantitative PET techniques used either i.v. $H_2{}^{15}O$ (3) or inhaled $C^{15}O_2$ (4), which is converted to $H_2{}^{15}O$ in the lungs by carbonic anhydrase. To calculate regional flow, only two measurements are required: the steady-state tracer concentration in the tissue, determined by PET, and the corresponding arterial tracer concentration, measured by blood sampling. This steady-state method, however, assumes that the partition coefficient of water is the same in healthy and diseased tissue and that the volume of distribution of water (V_d) is fixed. V_d is the proportion of a region of interest (ROI) in which the radioactive water is distributed, and a value of 0.5 corresponds to the ROI containing half the concentration of plasma. Because the steady-state method can lead to the underestimation of blood flow in heterogeneous tissues and where V_d is variable, a dynamic method was developed in which both flow and V_d are measured simultaneously (5–7).

Methods for quantifying regional flow by use of ^{15}O-labeled tracers have been well validated. Data obtained with PET were shown to correlate with other methods for measuring blood flow in the brain, myocardium, muscle, and kidney (8). The methods are widely used in the brain and heart, but fewer studies have been conducted in human tumors. The regional flow of brain tumors was shown to be variable with no consistent finding of whether it is higher or lower than in the normal brain (9–11). Breast tumors were shown to be better perfused than normal breast tissue, with the V_d being considerably higher (7). Other tracers are also being studied, such as ^{62}Cu-pyruvaldehyde bis(*N*-4-methylthiosemicarbazone) (PTSM; Ref.12), but are generally considered less useful in tumors than the ^{15}oxy-

Table 1 Tumors studied

Primary	Metastasis	*n*
Large bowel	Liver	13
	Lung	1
	Ovary	1
Liver		5
Carcinoid	Liver	1
Pancreas		4
	Liver	1
Anal		1
Stomach		1
Renal		2
Squamous cell carcinoma of the cheek		1
Endometrial sarcoma		1
Primitive neuro-ectodermal of shoulder		1
Bladder		1
Unknown	Liver	2
	Lung	1

gen-labeled molecules because they rely on metabolite trapping (8). Recently, studies have demonstrated the efficacy of using $H_2{}^{15}O$ PET (13–15) and ^{62}Cu-PTSM PET (12) measurements of blood flow for the early evaluation of novel antitumor agents.

For a method to be useful in the clinical evaluation of new anticancer agents, it must be quantitative and reproducible. $H_2{}^{15}O$ PET blood flow measurements have been shown to be reproducible in the brain (16), spleen (17), and heart (18). The lack of published data for human tumors and for the $C^{15}O_2$ inhalation method was the rationale behind the study reported here: an examination of the reproducibility of $C^{15}O_2$ PET measurements of regional flow in solid, predominantly intra-abdominal, tumors.

MATERIALS AND METHODS

Patients. The regional flow studies were approved by the ethical committee of the Imperial College School of Medicine, Hammersmith Hospital, London, United Kingdom. Permission to administer the radioactive tracers was obtained from the Administration of Radioactive Substances Advisory Committee of the United Kingdom. Patients with advanced, predominantly intra-abdominal malignancies were enrolled, and all gave written informed consent. Patients had a performance status $\leq$1. To minimize inter- and intrapatient variability in hepatic and portal venous flow and the effect of circadian variations in metabolism, patients in both studies fasted for a minimum of 4 h before scanning and were scanned at a similar time of day (19).

Patient Imaging. Labeled oxygen was produced by deuteron bombardment of a ^{14}N target in the United Kingdom Medical Research Council Scanditronix MC40 cyclotron, and was exposed to a nitrogen plus 1% CO_2 gas mixture to give $C^{15}O_2$ (20). The tracer was delivered at 4 MBq/ml and a flow rate of 500 ml/min via a light face mask (MC oxygen mask; Henleys Medical, Welwyn, United Kingdom) for 210 s, 30 s after the start of scanning. Patients were scanned for 10 min, and the data were collected into 30 time frames with the highest temporal sampling at the beginning of the scan (time frame 1 = 30 s; time frames 2–7 = 5 s; time frames 8–13 = 10 s; time frames 14–19 = 20 s; time frames 20–21 = 10 s; time frames 22–23 = 20 s; time frames 24–27 = 30 s; time frames 28–30 = 60 s). Imaging was performed on an ECAT 931-08/12 scanner (CTI PET Systems, Knoxville, TN) at the Hammersmith Hospital, London, United Kingdom, after insertion of an arterial line for blood sampling. Patient position was defined by X-ray simulation of the area of interest after localization of the tumor from a recent computed tomography scan. The axial field of view was 10.8 cm. A ^{68}Ge phantom was used for attenuation correction and calibration. During the flow scan, the radioactivity of arterial blood was monitored continually by passage through an on-line bismuth germinate detector calibrated with a well counter (21). Separate analysis of discrete blood samples enabled calibration of the radioactive counts.

PET Image Analysis. Sinogram data were reconstructed into tomographic images by use of filtered back-projection after transfer to a Sun SPARC Workstation (Sun Microsystems, Mountain View, CA). Voxel dimensions were 2.1 × 2.1 × 6.4 mm. Inspection of a recent computed tomography scan was used to assist the delineation of tumor and normal tissue regions. ROI

Table 2 Raw data[a]

	Tumor		Liver		Spleen		Kidney	
Patient	Flow[b]	V_d[c]	Flow	V_d	Flow	V_d	Flow	V_d
1	0.52	0.92						
2	0.65	1.07			0.19	0.95		
3	0.78	0.83	0.32	0.83			0.61	0.72
4	0.41	0.58						
5	0.65	0.76						
6	0.49	0.82			0.89	0.93	0.74	0.74
7	0.29	0.81						
8	0.17	0.63						
9	0.46	0.89	0.45	1.00	0.53	0.74		
10	0.39	0.76	0.34	0.75	0.98	0.79		
11	0.48	0.48						
12	0.42	0.85	0.46	0.84	0.55	0.86	0.69	0.65
13	0.32	0.84	0.44	0.92	1.05	0.77		
14	0.33	0.85	0.35	0.77	0.54	0.79		
15	0.37	0.60	0.04	0.21			0.98	0.62
16	0.63	0.78	0.55	0.73	1.03	0.74		
17	0.66	0.50						
18	0.35	0.72			0.97	0.78	0.58	0.5
19	0.97	0.82	0.53	0.74	0.49	0.75		
20	0.18	0.77	0.22	0.69	0.62	0.79	0.99	0.64
21	0.26	0.58	0.25	0.58	0.80	0.71	0.70	0.52
22	0.48	0.70	0.70	0.77	0.82	0.58		
23	0.38	0.71	0.40	0.7	1.11	0.73		
24	0.71	0.68	0.47	0.75	1.02	0.76		
25	0.40	0.71	0.48	0.72	0.92	0.72		
26	0.51	0.77	0.36	0.67	0.86	0.70		
27	0.85	0.75			1.17	0.70		
28	0.49	0.87	0.45	0.91	1.14	0.90	0.97	0.83
29	0.52	0.83	0.45	0.91	0.53	0.79		
30	0.64	1.04					1.04	0.76
31	0.27	0.40						
32	0.15	0.41						
33	0.33	0.54						
34	0.34	0.71						
35	0.34	0.80	0.37	0.91	0.77	0.90	1.69	0.68
36	0.47	0.70	0.57	0.70	0.88	0.73		
37	0.35	0.90	0.35	0.80	0.89	0.89	1.04	0.76

[a] Normal tissue data were not obtained for some patients because of an inadequate volume of normal tissue in the PET image.

[b] Regional flow in $ml_{blood}/min/ml_{tissue}$.

[c] V_d, volume of distribution, in ml_{blood}/ml_{tissue}.

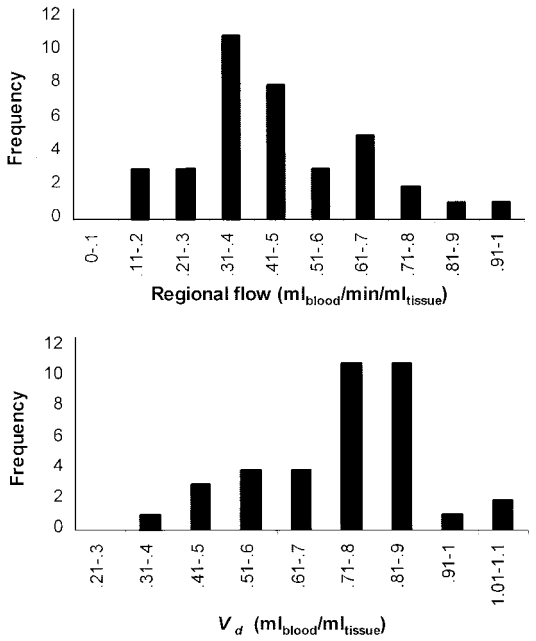

Fig. 1 Frequency histogram showing the distribution of tumor regional flow and volume of distribution (V_d) measured by $C^{15}O_2$ PET. Data are for 37 patients with advanced, predominantly intra-abdominal, malignancies.

were defined by use of Analyze image analysis software (Biomedical Imaging Resource, Mayo Foundation) on summed integral images (five plane minimum) rather than individual time frames. To ensure that only viable tumor was analyzed, tumor rims were defined by use of the computed tomography images and the regional flow scans. Once ROI were defined, mean pixel counts for each time frame were measured and plotted against midframe time to produce a time–activity curve. The same ROI were applied for the repeat studies by repositioning on an identical slice and by visual comparison.

Quantification of Regional Flow and V_d. Tissue and arterial ^{15}O concentrations were measured by use of the tomograph and bismuth germinate on-line detector, respectively. Data were calibrated with a well counter. Values for regional flow (ml$_{blood}$/min/ml$_{tissue}$) and the volume of tissue distribution of the tracer (V_d; ml$_{blood}$/ml$_{tissue}$) were obtained by use of the model originally described by Kety and Schmidt (22). The model requires a measure of the delay in tracer delivery between the point of sampling and its delivery to tissue, in addition to a measure of tracer dispersion in blood. The values for these parameters were adjusted to obtain the best fit to the model. After inhalation of $C^{15}O_2$, ^{15}O is transferred rapidly to the form of $H_2{}^{15}O$ by the action of carbonic anhydrase in the lung. Because $H_2{}^{15}O$ is a freely diffusible tracer, its behavior in tissue can be described by a single-tissue compartmental model:

$$dC_t(t)/dt = FC_a t(t) - (F/V_d + \lambda)C_t(t) \qquad (A)$$

Where $C_t(t)$ is the regional tissue concentration of $H_2{}^{15}O$ in Bq/ml as a function of time t; $C_a(t)$ is the arterial whole blood concentration of $H_2{}^{15}O$ in Bq/ml as a function of time; F is the regional flow in ml$_{blood}$/min/ml$_{tissue}$; V_d is the volume of distribution of water in ml$_{blood}$/ml$_{tissue}$; and $\lambda = 0.338$ min^{-1}, the decay constant of ^{15}O. The solution to the differential equation is given by:

$$C_t(t) = FC_a(t) \otimes exp[-(F/V_d + \lambda)t] \qquad (B)$$

Where $\otimes$ denotes the convolution; and $C_t(t)$ represents the tissue response to an arterial input function $C_a(t)$. When $C_a(t)$ and $C_t(t)$ are measured over time with dynamic PET, best estimates of both F and V_d can be obtained by standard nonlinear regression analysis (a simple least-squares algorithm) and minimizing the sum of squares of differences between the model output and the tissue data. Data were fitted by use of PET interactive data language (idl) software, and in-house Matlab (version 4.2; The Mathworks, Inc.) software was used for data analysis and presentation. It should be noted that $C_a(t)$ and $C_t(t)$ should not be corrected for decay because that has already been incorporated into equation B. In addition, parameters for the liver are only an index of regional flow and V_d because it has a dual blood supply

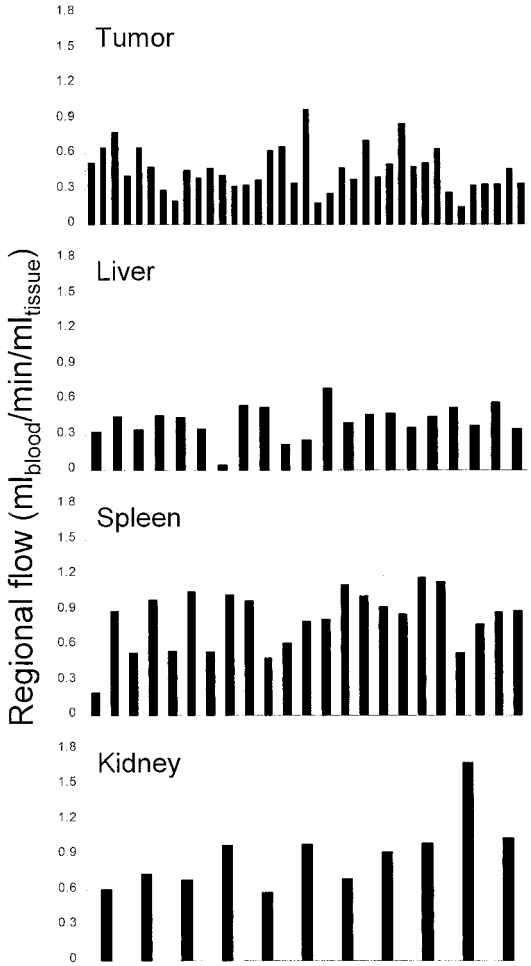

Fig. 2 Perfusion data in patients with advanced tumors. The *X axis* represents a consecutive series of patients.

Table 3 Summary of inter- and intrapatient variability in tumor and normal tissue regional flow

Parameter	Tissue	*n*	Mean ± SD	Range	CV[a] (%)	
					Interpatient	Intrapatient[b]
Flow ($ml_{blood}/min/ml_{tissue}$)	Tumor	37	0.46 ± 0.19	0.15–0.97	40	11
	Liver	21	0.41 ± 0.14	0.04–0.70	34	14
	Spleen	23	0.82 ± 0.25	0.19–1.17	31	9
	Kidney	11	0.90 ± 0.31	0.58–1.69	34	12
V_d (ml_{blood}/ml_{tissue})	Tumor	37	0.74 ± 0.15	0.40–1.07	21	6
	Liver	21	0.75 ± 0.16	0.21–1.00	21	13
	Spleen	23	0.78 ± 0.09	0.58–0.95	12	8
	Kidney	11	0.68 ± 0.11	0.50–0.88	18	3

[a] CV, coefficient of variation; V_d, volume of distribution.
[b] Intrapatient CV was studied in a subset of five (tumor) or four (liver, spleen) patients with measurement in the same patients made 1 week apart. For the kidney, both right and left kidneys were imaged in three patients on the same day.

from the hepatic artery and portal vein, and are thus only approximated by the one-compartment flow model (23).

Statistical Analyses. The variability in regional flow was expressed as a coefficient of variation (CV; SD/mean × 100, expressed as a percentage). Differences between the data obtained in paired scans on the same individual were tested by the Wilcoxon matched-pairs signed-rank test. The relationship between paired data were also tested with Spearman's correlation coefficient. A probability of $P < 0.05$ was used throughout to indicate a statistically significant result.

RESULTS

Interpatient Variability in Regional Flow. Table 1 summarizes the variety of tumors studied. Most of the tumors were intra-abdominal (35 of 37) and of gastrointestinal origin (31 of 37). Tumor flow and V_d data were obtained for all of the patients (Table 2; Fig. 1). For some of the patients, data were also obtained for ROI set in the liver, spleen, or kidney (Table 2; Fig. 2). The data are summarized in Table 3. Regional flow was highest in the kidney and lowest in the tumor and liver, both of which had similar levels of flow. There was more interpatient variability in tumor regional flow than in any of the normal tissues studied. Comparison of patients' weights, measured immediately before each scanning session, showed no changes in weight between sessions, providing some indication that patients had a similar volume status and level of hydration during their repeat scans. The V_d was similar in all of the tissues, with a similar degree of interpatient variability except in the spleen, where the level of variability was small.

Intrapatient Variability in Tissue Regional Flow. A subset of 5 of the 37 patients were scanned twice, 1 week apart, with no intervening therapy. Table 4 lists the tumor data obtained, which included measurements made in both non-necrotic and necrotic regions. As expected, the regional flow and V_d of necrotic regions were poor. Intrapatient variability was less than that seen between patients. There was no statistically significant difference in the paired scan data for regional flow or V_d. The relationships between the paired tumor regional flow and V_d data are shown in Fig. 3. Table 5 lists the repeat data for the normal tissues studied. Intrapatient variability was also less than interpatient variability for regional flow and V_d measured in normal liver, spleen, and kidney (Table 3). Again, there were no statistically significant differences between the paired data. ROI were drawn in the left and right kidney in three patients, and the regional flow and V_d data were obtained during a single scan. The intrapatient regional flow CV were similar (9–14%) for all of the tissues studied, but the CV for V_d varied from 3 to 13% and were smallest in the kidney.

DISCUSSION

For some conventional chemotherapeutic agents, the correlation between plasma drug levels and toxicity can be used to individualize and optimize drug dose levels (24). In these cases plasma levels form a surrogate for tumor drug doses. Tumors are heterogeneous, with variable perfusion (25, 26), which leads to uncertainty in the assessment of the relationship between plasma and tumor drug levels. This, along with the fact that many new anticancer agents lack the toxicity associated with conventional

Table 4 Intrapatient variability in tumor regional flow and volume of distribution

Patient	Imaged site	Necrotic	Regional flow ($ml_{blood}/min/ml_{tissue}$)		V_d[a] (ml_{blood}/ml_{tissue})	
			Reading 1	Reading 2	Reading 1	Reading 2
1	Liver	No	0.39	0.44	0.76	0.76
2	Lung	No	0.48	0.38	0.48	0.53
3	Liver	No	0.33	0.35	0.85	0.78
4	Liver	No	0.49	0.36	0.87	0.75
5	Liver	No	0.35	0.34	0.90	0.81
1	Liver	Yes	0.12	0.19	0.39	0.31
3	Liver	Yes	0.04	0.06	0.27	0.29

[a] V_d, volume of distribution.

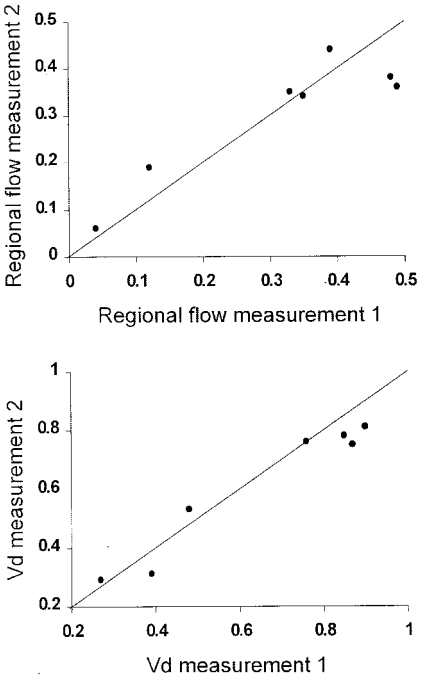

Fig. 3 Relationship between repeat measurements of regional flow (*top*) and volume of distribution (V_d; *bottom*) in patients with gastrointestinal tumors. The *lines* represent a theoretical exact correlation between the two measurements. There was a statistically significant correlation between the paired tumor regional flow ($\rho = 0.82$; $P = 0.023$) and V_d ($\rho = 0.89$; $P = 0.007$) data.

chemotherapeutic agents and also may target tumor vasculature, makes a reliable measurement of tumor perfusion attractive for Phase I studies of new antitumor agents. There is also interest in the relationship between tumor blood flow and patient response to therapy. Recent data showed that the combination of tumor ^{18}F-fluorodeoxyglucose metabolic and $H_2{}^{15}O$ blood flow measurements predicted disease-free survival in patients with locally advanced breast cancer undergoing chemotherapy (14). In addition, $H_2{}^{15}O$ blood flow measurements have been used to measure pharmacodynamic vascular changes in Phase I studies of the antiangiogenic agent endostatin (15) and the antivascular agent combretastatin A4-phospate (13).

Until recently, there has been a paucity of data on the use of PET to measure tumor vascular physiology *in vivo*. Table 6 summarizes some of the recent data obtained in patients with predominantly intra-abdominal cancer. Most of the studies listed in Table 6 involved the use of labeled water rather than carbon dioxide. Although injection of water is more widely used than inhalation of carbon dioxide for the administration of ^{15}O, Table 6 illustrates the similarity of the data obtained using the different approaches. In the study reported here, PET measurements of regional flow were variable among patients, in keeping with reports in the literature involving non-PET methods (25, 26). Regional flow was also more variable in the tumors than in the normal tissues studied, and higher regional flows were seen in the spleen and kidney than in either tumor or normal liver. The reduced regional flow measured in necrotic regions of tumors was expected and illustrates the sensitivity of PET for measurement of differences in regional flow.

The advantage of the dynamic over the steady-state method for measuring flow is that it allows for the V_d of the radiolabeled water and avoids the tendency to underestimate mean tumor flow in the presence of flow heterogeneity within a ROI. In normal breast, a V_d of 0.14 ml/ml was reported, with the low value attributed to the high fat content of the tissue (7). In breast tumor, a V_d of 0.56 and in cerebral gray matter a V_d of 0.86 have been reported (27). The V_d value of 0.74 ml_{blood}/ml_{tissue} for mainly intra-abdominal tumors falls within the range reported by others in other tissues (Table 6). Again, as for the regional flow data, the low V_d obtained in the necrotic areas of the tumors illustrates the sensitivity of PET for measurement of regional differences in vascular hemodynamic parameters.

No term was used to account for radioactivity from the blood volume in either the imaged tissue or adjacent vascular structures (spillover). The lack of a term might lead to an overestimate of the measurements of regional flow and V_d in highly vascularized tumors or in tumors close to major blood vessels. This contrasts with cardiac studies in which imaging is carried out adjacent to vascular structures and a spillover term is required. A term is not generally applied to tumor PET flow studies when the tumors imaged are not near highly vascularized structures, as was the case in the work reported here. In the study by Hoekstra *et al.* (28) of lung tumors, however, a single-compartment model was used both with and without an arterial blood volume component. Better fits to the data were obtained with the incorporation of a blood volume component. This might be attributable to the highly vascular nature of the surrounding normal lung tissue, resulting in a significant spillover term. However, it might be of interest, therefore, to explore the use of the term spillover in future PET studies of regional flow in tumors.

This study has shown that the measurement of regional flow by $C^{15}O_2$ PET is a reproducible method in patients with solid, predominantly intra-abdominal, tumors. The intrapatient reproducibility is also in keeping with that reported for the use of $H_2{}^{15}O$ PET to measure cerebral (16) and spleenic (17) blood flow. Recently ^{62}Cu-PTSM measurements of tumor flow were

Table 5 Intrapatient variability in normal tissue regional flow and volume of distribution

	Regional flow ($ml_{blood}/min/ml_{tissue}$)		$V_d{}^a$ (ml_{blood}/ml_{tissue})	
Organ	Reading 1	Reading 2	Reading 1	Reading 2
Liver	0.34	0.49	0.75	0.81
	0.35	0.46	0.77	0.51
	0.45	0.46	0.91	0.75
	0.35	0.30	0.80	0.76
Spleen	0.98	1.13	0.79	0.79
	0.54	0.63	0.79	0.59
	1.14	1.05	0.90	0.81
	0.89	0.80	0.89	0.85
Kidney	0.61	0.98	0.72	0.67
	0.98	0.98	0.62	0.62
	0.97	0.92	0.83	0.81

[a] V_d, volume of distribution.

Table 6 Between-study comparison of $H_2{}^{15}O$ PET measurements of regional flow and volume of distribution

Study	Site	Patients	Flow ($ml_{blood}/min/ml_{tissue}$)	V_d[a] (ml_{blood}/ml_{tissue})
Wilson *et al.*, 1992 (7)	Normal breast	20	0.06 ± 0.01	0.14 ± 0.05
Mankoff *et al.*, 2002 (14)	Normal breast	37	0.06	0.18
Wilson *et al.*, 1992 (7)	Breast tumor	20	0.30 ± 0.17	0.56 ± 0.15
Mankoff *et al.*, 2002 (14)	Breast tumor	37	0.32	0.58
Yamaguchi *et al.*, 2000 (30)[b]	CRC liver metastases	15	0.36 ± 0.04[c]	
Herbst *et al.*, 2002 (15)	Advanced solid tumors	25	0.36 ± 0.27	
Lehtio *et al.*, 2001 (31)	Head and neck tumors	8	0.38 ± 0.15	
This study[b]	Intra-abdominal tumors	37	0.46 ± 0.19	0.74 ± 0.15
Anderson *et al.*, 2003 (13)	Intra-abdominal tumors	13	0.54 ± 0.46	0.78 ± 0.21
Hoekstra *et al.*, 2002 (28)	NSCLC	10	0.59 ± 0.37	0.63 ± 0.10
Anderson *et al.*, 2003 (13)	Normal spleen	13	1.05 ± 0.34	0.88 ± 0.13
Anderson *et al.*, 2003 (13)	Normal kidney	13	1.32 ± 0.30	0.77 ± 0.08

[a] V_d, volume of distribution; CRC, colorectal cancer; NSCLC, non-small cell lung cancer.
[b] $C^{15}O_2$ used rather than $H_2{}^{15}O$.
[c] Regional flow was 0.53 ± 0.17 $ml_{blood}/min/ml_{tissue}$ in 5 tumors with high vascularization, 0.32 ± 0.04 in 10 tumors with similar vascularization to normal, and 0.32 ± 0.06 in 7 tumors with poor vascularization.

also shown to be reproducible when a single patient with colorectal liver metastases was scanned on three separate occasions (29). In the study reported here, data were also available for within-scan intrapatient variability. A similar level of variability was seen for the kidney regional flow data (CV = 12%), where the variability between right and left kidney data obtained during the same scan were compared, as for the between-scan intrapatient variability in the other tissues examined (CV = 11–14%). These data suggest that machine, set-up, and analysis errors are minimal for PET flow studies in intra-abdominal malignancies. The within-scan intrapatient variability in V_d was smaller (kidney CV = 3%) than the between-scan intrapatient variability in the other tissues studied (CV = 6–13%) and suggests that the machine/set-up/analysis errors might contribute approximately half of the measured intrapatient variability.

The conclusion from this study is that PET measurements of regional flow are reproducible in patients with advanced, predominantly intra-abdominal, tumors. This study supports the continuing development of PET measurements of tumor blood flow for the pharmacodynamic evaluation of antiangiogenic/vascular agents.

REFERENCES

1. Kety, S. S. Theory of blood-tissue exchange and its application to measurement of blood flow. Methods Med. Res., *8:* 228–236, 1960.

2. Kety, S. S. The theory and application of the exchange of inert gas at the lung and tissues. Pharmacol. Rev., *1:* 1–41, 1951.

3. Herscovitch, P., Markham, J., and Raichle, M. E. Brain blood flow measured with intravenous H2(15)O. I. Theory and error analysis. J. Nucl. Med., *24:* 782–789, 1983.

4. Frackowiak, R. S., Jones, T., Lenzi, G. L., and Heather, J. D. Regional cerebral oxygen utilization and blood flow in normal man using oxygen-15 and positron emission tomography. Acta Neurol. Scand., *62:* 336–344, 1980.

5. Lammertsma, A. A., Cunningham, V. J., Deiber, M. P., Heather, J. D., Bloomfield, P. M., Nutt, J., Frackowiak, R. S., and Jones, T. Combination of dynamic and integral methods for generating reproducible functional CBF images. J. Cereb. Blood Flow Metab., *10:* 675–686, 1990.

6. Araujo, L. I., Lammertsma, A. A., Rhodes, C. G., McFalls, E. O., Iida, H., Rechavia, E., Galassi, A., De Silva, R., Jones, T., and Maseri, A. Noninvasive quantification of regional myocardial blood flow in coronary artery disease with oxygen-15-labeled carbon dioxide inhalation and positron emission tomography. Circulation, *83:* 875–885, 1991.

7. Wilson, C. B., Lammertsma, A. A., McKenzie, C. G., Sikora, K., and Jones, T. Measurements of blood flow and exchanging water space in breast tumors using positron emission tomography: a rapid and noninvasive dynamic method. Cancer Res., *52:* 1592–1597, 1992.

8. Anderson, H., and Price, P. Clinical measurement of blood flow in tumours using positron emission tomography: a review. Nucl. Med. Commun., *23:* 131–138, 2002.

9. Mineura, K., Sasajima, T., Itoh, Y., Sasajima, H., Kowada, M., Tomura, N., Uesaka, Y., Ogawa, T., Hatazawa, J., and Uemura, K. Blood flow and metabolism of central neurocytoma: a positron emission tomography study. Cancer (Phila.), *76:* 1224–1232, 1995.

10. Mineura, K., Shioya, H., Kowada, M., Ogawa, T., Hatazawa, J., and Uemura, K. Blood flow and metabolism of oligodendrogliomas: a positron emission tomography study with kinetic analysis of ^{18}F-fluorodeoxyglucose. J. Neurooncol., *43:* 49–57, 1999.

11. Lassen, U., Andersen, P., Daugaard, G., Holm, S., Jensen, M., Svarer, C., Poulsen, H. S., and Paulson, O. B. Metabolic and hemodynamic evaluation of brain metastases from small cell lung cancer with positron emission tomography. Clin. Cancer Res., *4:* 2591–2597, 1998.

12. Burke, D., Davies, M. M., Zweit, J., Flower, M. A., Ott, R. J., Dworkin, M. J., Glover, C., McCready, V. R., Carnochan, P., and Allen-Mersh, T. G. Continuous angiotensin II infusion increases tumour: normal blood flow ratio in colo-rectal liver metastases. Br. J. Cancer, *85:* 1640–1645, 2001.

13. Anderson, H. L., Yap, J. T., Miller, M. P., Robbins, A., Jones, T., and Price, P. M. Assessment of pharmacodynamic vascular response in a phase I trial of combretastatin A4 phosphate. J. Clin. Oncol., *21:* 2823–2830, 2003.

14. Mankoff, D. A., Dunnwald, L. K., Gralow, J. R., Ellis, G. K., Charlop, A., Lawton, T. J., Schubert, E. K., Tseng, J., and Livingston, R. B. Blood flow and metabolism in locally advanced breast cancer: relationship to response to therapy. J. Nucl. Med., *43:* 500–509, 2002.

15. Herbst, R. S., Mullani, N. A., Davis, D. W., Hess, K. R., McConkey, D. J., Charnsangavej, C., O'Reilly, M. S., Kim, H. W., Baker, C., Roach, J., Ellis, L. M., Rashid, A., Pluda, J., Bucana, C., Madden, T. L., Tran, H. T., and Abbruzzese, J. L. Development of biologic markers of response and assessment of antiangiogenic activity in a clinical trial of human recombinant endostatin. J. Clin. Oncol., *20:* 3804–3814, 2002.

16. Matthew, E., Andreason, P., Carson, R. E., Herscovitch, P., Pettigrew, K., Cohen, R., King, C., Johanson, C. E., and Paul, S. M. Reproducibility of resting cerebral blood flow measurements with H2(15)O positron emission tomography in humans. J. Cereb. Blood Flow. Metab., *13:* 748–754, 1993.

17. Taniguch, H., Kunishima, S., Koh, T., Oguro, A., and Yamagishi, H. Reproducibility of repeated human regional splenic blood flow measurements using [^{15}O] water and positron emission tomography. Nucl. Med. Commun., *22:* 755–757, 2001.

18. Iida, H., Yokoyama, I., Agostini, D., Banno, T., Kato, T., Ito, K., Kuwabara, Y., Oda, Y., Otake, T., Tamura, Y., Tadamura, E., Yoshida, T., and Tamaki, N. Quantitative assessment of regional myocardial blood flow using oxygen-15-labelled water and positron emission tomography: a multicentre evaluation in Japan. Eur. J. Nucl. Med., *27:* 192–201, 2000.

19. Torizuka, T., Clavo, A. C., and Wahl, R. L. Effect of hyperglycemia on in vitro tumor uptake of tritiated FDG, thymidine, L-methionine and L-leucine. J. Nucl. Med., *38:* 382–386, 1997.

20. Rhodes, C. G., Lenzi, G. L., Frackowiak, R. S., Jones, T., and Pozzilli, C. Measurement of CBF and CMRO2 using the continuous inhalation of C^{15}O$_2$ and ^{15}O. Experimental validation using CO_2 reactivity in the anaesthetised dog. J. Neurol. Sci., *50:* 381–389, 1981.

21. Ranicar, A. S., Williams, C. W., Schnorr, L., Clark, J. C., Rhodes, C. G., Bloomfield, P. M., and Jones, T. The on-line monitoring of continuously withdrawn arterial blood during PET studies using a single BGO/photomultiplier assembly and non-stick tubing. Med. Prog. Technol., *17:* 259–264, 1991.

22. Kety, S. S., and Schmidt, C. F. The nitrous oxide method for the quantitative determination of cerebral blood flow in man: theory, procedure and normal values. J. Clin. Investig., *27:* 476–486, 1948.

23. Ziegler, S. I., Haberkorn, U., Byrne, H., Tong, C., Kaja, S., Richolt, J. A., Schosser, R., Krieter, H., Lammertsma, A. A., and Price, P. Measurement of liver blood flow using oxygen-15 labelled water and dynamic positron emission tomography: limitations of model description. Eur. J. Nucl. Med., *23:* 169–177, 1996.

24. Canal, P., Chatelut, E., and Guichard, S. Practical treatment guide for dose individualisation in cancer chemotherapy. Drugs, *56:* 1019–1038, 1998.

25. Chaplin, D. J., and Hill, S. A. Temporal heterogeneity in microregional erythrocyte flux in experimental solid tumours. Br. J. Cancer, *71:* 1210–1213, 1995.

26. Vaupel, P., Kallinowski, F., and Okunieff, P. Blood flow, oxygen and nutrient supply, and metabolic microenvironment of human tumors: a review. Cancer Res., *49:* 6449–6465, 1989.

27. Lammertsma, A. A., Martin, A. J., Friston, K. J., and Jones, T. *In vivo* measurement of the volume of distribution of water in cerebral grey matter: effects on the calculation of regional cerebral blood flow. J. Cereb. Blood Flow Metab., *12:* 291–295, 1992.

28. Hoekstra, C. J., Stroobants, S. G., Hoekstra, O. S., Smit, E. F., Vansteenkiste, J. F., and Lammertsma, A. A. Measurement of perfusion in stage IIIA-N2 non-small cell lung cancer using H(2)(15)O and positron emission tomography. Clin. Cancer Res., *8:* 2109–2115, 2002.

29. Flower, M. A., Zweit, J., Hall, A. D., Burke, D., Davies, M. M., Dworkin, M. J., Young, H. E., Mundy, J., Ott, R. J., McCready, V. R., Carnochan, P., and Allen-Mersh, T. G. ^{62}Cu-PTSM and PET used for the assessment of angiotensin II-induced blood flow changes in patients with colorectal liver metastases. Eur. J. Nucl. Med., *28:* 99–103, 2001.

30. Yamaguchi, A., Taniguchi, H., Kunishima, S., Koh, T., and Yamagishi, H. Correlation between angiographically assessed vascularity and blood flow in hepatic metastases in patients with colorectal carcinoma. Cancer (Phila.), *89:* 1236–1244, 2000.

31. Lehtio, K., Oikonen, V., Gronroos, T., Eskola, O., Kalliokoski, K., Bergman, J., Solin, O., Grenman, R., Nuutila, P., and Minn, H. Imaging of blood flow and hypoxia in head and neck cancer: initial evaluation with [(15)O]H(2)O and [(18)F]fluoroerythronitroimidazole PET. J. Nucl. Med., *42:* 1643–1652, 2001.